Wave effects in gravitational lensing of electromagnetic radiation

Shuji Deguchi
Department of Physics, University of Illinois at Urbana-Champaign, 1110 West Green Street, Urbana, Illinois 61801

William D. Watson
Department of Physics and Department of Astronomy, University of Illinois at Urbana-Champaign, 1110 West Green Street, Urbana, Illinois 61801

(Received 27 January 1986)

Wave effects in the gravitational lensing of electromagnetic radiation by compact objects in astrophysics are treated. In the regime where the influence of diffraction is severe, solutions of the wave equation appropriate for lensing in astrophysics (which is of the form of the Schrödinger equation for Coulomb scattering) are obtained. In the WKB regime, previous formulations are refined and extended to the case in which a part of the source is directly behind the lensing mass. Wave effects tend to be largest for this geometry which requires that radiation at a caustic be treated. The autocorrelation function of the electric field and the related frequency dependence of the radiation are emphasized, in addition to the diffraction pattern, to measure the deviations from the solutions obtained in the approximation of geometrical optics. In contrast, gravitational lensing is independent of frequency in the usual treatment which is based upon geometrical optics. Numerical computations are performed to indicate how the wave effects depend upon the relevant parameters including especially the size of the source. Wave effects are most significant at radio frequencies and for lensing by stellar and planetary masses. The importance of wave effects is governed by the ratio of the Schwarzschild radius of the lensing mass to the wavelength of the radiation.

I. INTRODUCTION

The cases (some 5—10 at present) in which gravitational lensing has been identified in astronomy have all involved a distant lens having the mass of a galaxy. It has been recognized that potentially detectable effects of gravitational lensing occur even for masses as small as that of a single star.[1] Lensing by galactic masses is recognized by the two or more images, separated by arcseconds in angular location, that can be identified. In lensing by a stellar mass, the predicted separation of the images is not large enough to be resolved. The interest in these lenses has thus centered on their ability to brighten the single observable image of the source. Unfortunately, distinguishing characteristics for this type of lensing that would make it identifiable are not so readily available as in the case of lensing by galaxies. For example, detecting variations in the brightness caused by the relative motion of the source, the lens, and Earth requires about 100 years for typical parameters when the lens is at cosmological distances. The time scale can be much shorter (roughly days) for lensing masses within our own Galaxy. Here, however, the probability for lensing along a particular line of sight is quite small and the infrequent changes in brightness (less than about a factor of 2) that might be expected for a small fraction of sources is likely to be overshadowed by unpredictable variations due to other causes.

The foregoing description of gravitational lensing has been based on the approximation of geometrical optics. For lensing by solar and planetary masses, wave effects might be detectable[2] and provide additional characteristic properties necessary to identify gravitational lensing by such objects. An evaluation of the mutual coherence that occurs has been performed using a WKB approximation for a restricted range of the possible geometries.[3] We[4] have previously obtained the appropriate wave equation which is of the form of the Schrödinger equation for Coulomb scattering and have evaluated the solutions for an infinitely distant source (incident plane waves) to obtain the diffraction pattern. A key consideration for gravitational lensing by objects of stellar mass can be the finite size of the source (incident waves with curvature) and is not covered by our previous treatment.

The characteristic angular scale in gravitational lensing by a point mass M is

$$\theta_0 \simeq \left[\frac{4GM}{c^2L}\right]^{1/2} \simeq 10^{-3}[(M/M_0)(10\ \text{kpc}/L)]^{1/2}\text{arcsec}\ , \tag{1}$$

where L is roughly the distance to the lensing mass unless the lens is much closer to the source than to the observer [see Eq. (16) for an exact expression] and M_0 is the mass of the Sun. Lensing effects ordinarily are expected to be significant only when the source, lens, and observer are aligned within approximately the angle θ_0. When the angular size of the source is greater than about θ_0, the relative influence of the lensing is reduced. Although this may well be the case for lensing masses with $M \lesssim M_0$ and located outside the Galaxy ($L > 10$ kpc), the possible

detection of quite small alterations in the properties of the radiation is not an unreasonable expectation. Wave effects in gravitational lensing by a point mass depend upon the parameter

$$y = 4\pi GM/c^2\lambda = 2\times 10^6 (M/M_0)/\lambda(\text{cm}) \quad (2)$$

which measures the number of Fresnel zones that are contributing to the lensing. It is essentially the square of the ratio of θ_0 to the Fresnel angle $(\lambda/L)^{1/2}$ for a wavelength λ of the radiation. Except for a factor of 2π, it also is the ratio of the Schwarzschild radius to the wavelength λ for the radiation. When $y \simeq \infty$ geometrical optics applies and when $y \gg 1$ the WKB approximation is expected to be accurate. When $y \simeq 1$ severe effects of diffraction should occur and less approximate solutions of the wave equation are necessary.

In addition to assessing the alterations in the properties of radiation caused by objects of substellar mass, it is also desirable to determine precisely how these effects depend on the angle θ between the lensing mass and the source as seen by the observer. In benchmark estimates of the probability for gravitational lensing along a particular line of sight, appreciable effects ordinarily are assumed to occur only for $\theta \lesssim \theta_0$. This probability is quite low ($\simeq 10^{-6}$) for lensing due to masses without our own Galaxy but can be near unity for lensing masses at cosmological distances if the mass density of the Universe is near the critical value for closure. The analogous probability for lensing by single stars when radiation passes through other galaxies or clusters of galaxies can be much greater than for our own Galaxy and in some cases may also be near unity. Studies of gravitational lensing by compact objects $M \lesssim M_0$ may be useful in delineating the amount of dark matter in the Universe in the form of such objects just as they have been for masses $M \gtrsim M_0$ (Ref. 1).

To assess the wave effects in gravitational lensing, we consider the autocorrelation function $\Gamma(T)$ involving the time average of the electric fields E (expressed in complex form) at times t and $t+T$:

$$\Gamma(T) = \langle E(t)E^*(t+T) + E^*(t)E(t+T)\rangle/2 \; . \quad (3)$$

This seems to be the quantity that instruments at radio frequencies ordinarily are designed to measure directly with greatest accuracy. It is also the quantity on which previous studies[2,3] have focused. Related effects introduced by a wave treatment are the diffraction pattern in space [that is, $\Gamma(0)$ as a function of spatial location] and a wavelength dependence of the brightening of the source by the lens [that is, $\Gamma(0)$ as a function of wavelength]. The time source for variations in these quantities due to the relative motions can be significantly shortened because there can be many (depending upon the value of y) diffraction peaks within the angle θ_0.

In Sec. II of this paper we extend our previous investigation and obtain solutions of the wave equation for radiation emitted by a point source that is gravitationally lensed by a point mass. By integrating these solutions over the surfaces of sources, we then assess the properties of lensed radiation in the diffraction regime ($y \simeq 1$) for sources of finite size. In Sec. III we extend the previous WKB formulation by deducing a relevant phase factor, by obtaining solutions appropriate for the important case in which a portion of the source is located directly behind the lensing mass, and by integrating these WKB solutions over a nonuniform (Gaussian) as well as uniform brightness distribution at the source. The results of numerical computations are presented to indicate the resulting wave effects for representative values of the parameters. Observational considerations are mentioned in Sec. IV.

II. SOLUTION OF THE "FULL" WAVE EQUATION

We showed previously[4] that, in the context of gravitational lensing in astrophysics, the propagation of electromagnetic radiation in the presence of the gravitational field of a compact object can be described to an excellent approximation by a scalar wave equation of the same form as the time-independent Schrödinger equation for Coulomb scattering. This is based upon the weak-field limit for the gravitation and ignoring the finite size of the lensing mass. For significant effects of gravitational lensing, the characteristic angular size of the region around the lensing mass from which the incident wave is scattered is the θ_0 of Eq. (1). Although this angle is exceedingly small, for distances characteristic of the Galaxy or greater it still corresponds to an impact parameter, or $L\theta_0 = (4GML/c^2)^{1/2}$ in the notation of Eq. (1), that is very much greater than the radii of compact astronomical objects with masses $M \lesssim M_0$ (i.e., ordinary stars, while dwarf stars, planets). In terms of the familiar partial-wave decomposition of the Schrödinger equation,[5] the radial part of the solution associated with the partial wave l will have a negligible amplitude at distances closer to the lensing mass than $b_l \simeq [l(l+1)]^{1/2}\lambda/2\pi$. By far, most of the partial waves involved in the lensing (i.e., those with $b_l \lesssim L\theta_0$) have b_l much greater than the physical radius of the compact lensing mass. Further, gravitational lensing of astrophysical interest is significant only for $\theta_0 \ll 1$ which is the forward-scattering regime and is thus dominated by partial waves having the larger l values. Ignoring the finite size of the mass and treating it as a "point mass" is then expected to be an excellent approximation. If $\lambda/L\theta_0$ were not small or if large scattering angles were of interest, this approximation would fail. If the lensing mass is a black hole, the weak-field approximation is still satisfied for essentially all of the partial waves that contribute significantly because $L\theta_0$ is much greater than the Schwarzschild radius, which measures the region in which the weak-field approximation fails. The foregoing reasoning remains valid.[6] A *scalar* wave equation results because effects involving the polarization of the radiation are negligible in the weak-field approximation.

We obtained solutions[4] only for a source at infinite distances; that is, for incident plane waves. We now obtain solutions for a point source at finite distances. These solutions are then integrated over the source distribution to assess the influence of the finite size of the source.

A. Similarity solution for the wave equation

As shown previously[4] the relevant wave equation allows the usual separation of the space $\mathbf{r}$ and time t so that a

component of the electric field with angular frequency ω can be expressed as

$$E(t,\mathbf{r})=\psi(\mathbf{r})e^{-i\omega t} . \tag{4}$$

For a point source of radiation at the origin and a point mass M at the location $\mathbf{r}_0$, the equation for $\psi(\mathbf{r})$ is obtained by a straightforward extension of previous work:[4]

$$\Delta\psi+k^2[1+4GM/(c^2|\mathbf{r}-\mathbf{r}_0|)]\psi=-4\pi\delta(\mathbf{r}) , \tag{5}$$

where G is the constant for gravitation and k is the wave number for the radiation:

$$k\equiv\omega/c . \tag{6}$$

As is generally recognized in gravitational lensing, effects due to including polarization appear only in higher order because of the very small angular deflections and the weak-field approximation.

The solution near the light source must be the free spherical wave

$$\psi\rightarrow\psi_+=\frac{1}{r}\exp(ikr) \quad \text{as} \quad r\rightarrow 0 , \tag{7}$$

where the function ψ_+ satisfies

$$\Delta\psi_++k^2\psi_+=-4\pi\delta(\mathbf{r}) . \tag{8}$$

It is thus natural to seek a solution of the form

$$\psi=H(\mathbf{r})\psi_+ . \tag{9}$$

Inserting Eq. (9) into Eq. (5) gives the differential equation for H:

$$\frac{\partial^2H}{\partial r^2}+2ik\frac{\partial H}{\partial r}+\frac{1}{r^2}\frac{1}{\sin\phi}\frac{\partial}{\partial\phi}\left[\sin\phi\frac{\partial}{\partial\phi}H\right]+4k^2GMH/(c^2|\mathbf{r}-\mathbf{r}_0|)=0 , \tag{10}$$

where ϕ is the angle in spherical coordinates shown in Fig. 1. Of course,

$$|H|\rightarrow 1 \tag{11}$$

as $r\rightarrow 0$.

We now make the following two approximations that are applicable for gravitational lensing in astrophysics. First, the second-order derivative with respect to r is neglected. Because the scale length for the variation in H is of the order of radius r, the second-order derivative is much smaller than the first-order term. That is,

$$\left|\frac{\partial^2H}{\partial r^2}\right|\ll\left|2ik\frac{\partial H}{\partial r}\right| . \tag{12a}$$

Second, the angle ϕ is considered to be small so that

$$\sin\phi\sim\phi . \tag{12b}$$

Even for masses as large as that of an entire Galaxy, the characteristic angular deflections are only several arcseconds. By introducing the transformation

$$H=F(r,\phi)e^{iy\ln r} , \tag{13}$$

Eq. (10) with approximations (12a) and (12b) can be written

$$2ik\frac{\partial F}{\partial r}+\frac{1}{r^2}\frac{1}{\phi}\frac{\partial}{\partial\phi}\left[\phi\frac{\partial}{\partial\phi}F\right]+\frac{4k^2GMr_0}{c^2r|\mathbf{r}-\mathbf{r}_0|}F=0 . \tag{14}$$

We now define

$$x\equiv(\theta/\theta_0)^2 , \tag{15a}$$

$$y\equiv 2GMk/c^2 , \tag{15b}$$

and

$$\theta_0^2\equiv\frac{4GM}{c^2(r-r_0)}\frac{r_0}{r} , \tag{16}$$

where θ is the angle between the lens and the source as shown in Fig. 1. In the approximation of small angles

$$r_0\phi=(r-r_0)\theta . \tag{17}$$

We now try a solution for F that is a function of x alone. With

$$\partial x/\partial\phi=2x/\phi \tag{18}$$

and

$$\partial x/\partial r=-xr_0/[(r-r_0)r] , \tag{19}$$

Eq. (14) becomes

$$x\frac{\partial^2F}{\partial x^2}+\frac{\partial F}{\partial x}(1-iyx)+y^2F=0 . \tag{20}$$

Equation (20) is a standard form of the differential equation which has the confluent hypergeometric function $F_c(a,b,Z)$ as its solution:

$$F=\exp\left[\frac{\pi}{2}y\right]\Gamma(1-iy)F_c(iy,1,iyx) . \tag{21}$$

Here, the normalization is taken as $HH^*\rightarrow 1$ at $r\rightarrow\infty$. The overall solution to the wave equation (5) is then

$$\psi=\frac{1}{r}\exp\left[ikr+iy\ln r+\frac{\pi}{2}y\right]\Gamma(1-iy)F_c(iy,1,iyx) . \tag{22}$$

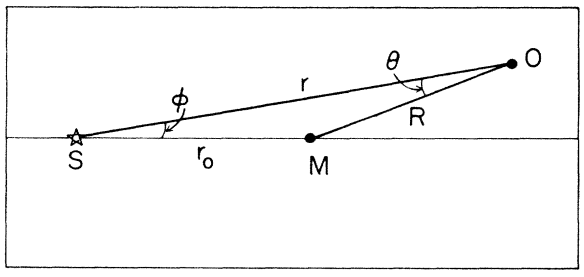

FIG. 1. Geometry for the source S, lensing mass M, and observer O. The angles θ and ϕ, and the distances r, r_0, and R are indicated.

If we compare this with our previous results for incident plane waves,[4] the differences are that the original wave is expressed by a spherical wave (as expected for the finite distance source) and that the angle parameter θ_0^2 is multiplied by the factor (r_0/r) to obtain that given in Eq. (16). Apart from a phase factor, the dimensionless spatial variable x describes the influence of gravitational lensing just as in the Liebes-Refsdal solution for the approximation of geometrical optics. The transformation found above in going from incident plane waves to incident spherical waves is the same as that which has been recognized in the context of wave propagation in random media.[7]

The brightness of the source is amplified by the factor

$$\psi\psi^*/(\psi_+\psi_+^*)=\frac{2\pi y}{(1-e^{-2\pi y})}F_cF_c^* \ . \tag{23}$$

As shown previously,[4] this amplification is the same as that of the Liebes-Refsdal solution if the geometrical optics limit is taken by allowing the frequency parameter y to be much larger than one and by averaging over the oscillations.

In summary, the effect of the gravitational attraction of a point mass is to introduce a confluent hypergeometric function into the description of the electric field. This is the case regardless of whether the incident wave is a plane wave or has curvature. As the source becomes infinitely distant so that $r_0/r\rightarrow 1$, the confluent hypergeometric function of the solution here approaches that obtained for a source at infinity.[4]

B. Evaluation of the properties of the radiation for objects of finite size

For an incoherent source of finite size, the solutions found for a point source can be integrated over the brightness distribution $L(S)$ at the surface S of the source to obtain the autocorrelation function defined in Eq. (3) at a location beyond the lensing mass:[8]

$$\Gamma(T)=\frac{1}{2\Delta\omega}\int L(S)\cos(\omega T)\psi^*\psi\, dS\, d\omega \ . \tag{24}$$

Here, the integral is over the surface of the source and the bandwidth $\Delta\omega$ within which the detector has uniform response. For simplicity, any dependence on frequency in $L(S)$ will be ignored. Because ψ depends only on one spatial dimension (through x) and the parameter y, it is convenient to express Eq. (24) in the form

$$\Gamma(\tau)=\frac{R^2\theta_0^{\,2}}{4\Delta y}\int L(x,\alpha)\psi^*(x,y)\psi(x,y)\cos(y\tau)dx\, d\alpha\, dy \ , \tag{25}$$

where

$$\tau=\frac{\omega T}{y} \ , \tag{26}$$

the distance to the source is R (which is approximately r) and the angle α is the azimuthal angle perpendicular to θ in Fig. 1 that describes locations on the source.

In this section, the emphasis is on parameters for which the effects of diffraction are large—that is, values of y which are not large in comparison with unity. At radio frequencies, instruments ordinarily have bandwidths such that $(\Delta\omega/\omega)\ll 1$. We thus utilize an approximation appropriate for dimensionless bandwidths $\Delta y\ll 1$. Only the first two terms in the Taylor series for $(\psi^*\psi)$ are retained:

$$(\psi^*\psi)\simeq(\psi^*\psi)_0+(y-y_0)\frac{\partial}{\partial y}(\psi^*\psi)_0 \ , \tag{27}$$

where the subscript denotes an evaluation at the center y_0 of the band. Inserting Eq. (27) into the expression for $\Gamma(\tau)$ yields

$$\Gamma(\tau)=B_0(\tau)\cos(y_0\tau)+B_2(\tau)\sin(y_0\tau) \tag{28}$$

for

$$B_0(\tau)=\tfrac{1}{4}R^2\theta_0^{\,2}g(\tau)\int L(x,\alpha)(\psi^*\psi)_0 dx\, d\alpha \tag{29a}$$

and

$$B_2(\tau)=\tfrac{1}{4}R^2\theta_0^{\,2}(\Delta y/2)g_2(\tau) \times\int L(x,\alpha)\left[\frac{\partial(\psi^*\psi)}{\partial y}\right]_0 dx\, d\alpha \ , \tag{29b}$$

where

$$g(\tau)=\sin(\tau\Delta y/2)/(\tau\Delta y/2) \tag{30a}$$

and

$$g_2(\tau)=[\cos(\tau\Delta y/2)-\sin(\tau\Delta y/2)/(\tau\Delta y/2)]/(\tau\Delta y/2) \ . \tag{30b}$$

A term similar to that involving B_0 in Eq. (28) would be present in the absence of the lensing mass and would have the same dependence on τ. Lensing does, however, alter the magnitude of this term and introduces an additional spatial variation. In fact, for $\tau=0$ this term describes the brightness of the source and thus represents a diffraction pattern. The influence of lensing on the τ dependence of $\Gamma(\tau)$ comes from the term involving B_2. While the function g is symmetric in τ, g_2 is antisymmetric and has a maximum in its absolute magnitude at $(y\Delta\tau/2)\simeq 2.3$. These functions are displayed in Fig. 2.

The ratio B_2/B_0 is thus a measure of the alteration of $\Gamma(\tau)$ versus τ caused by gravitational lensing for a particular observing location. It is then convenient to define

$$K\equiv\int L(x,y)\left[\frac{\partial(\psi^*\psi)}{\partial y}\right]_0 dx\, d\alpha/\int L(x,y)(\psi^*\psi)_0 dx\, d\alpha \ . \tag{31}$$

The function K does not depend on the parameters of the telescope such as bandwidth. Figure 3 shows K as a function of the variable $t_c\equiv(\theta_c/\theta_0)$, where θ_c is the angle θ in Fig. 1 at the center of the source. Calculations are performed for several values of the parameter $(\Delta\theta/\theta_0)\equiv\Delta t$, where $2\Delta\theta$ is the angular diameter of the source, which is treated as a circular disk with a uniform brightness distribution. At fixed (θ_c/θ_0), the function K approaches π as

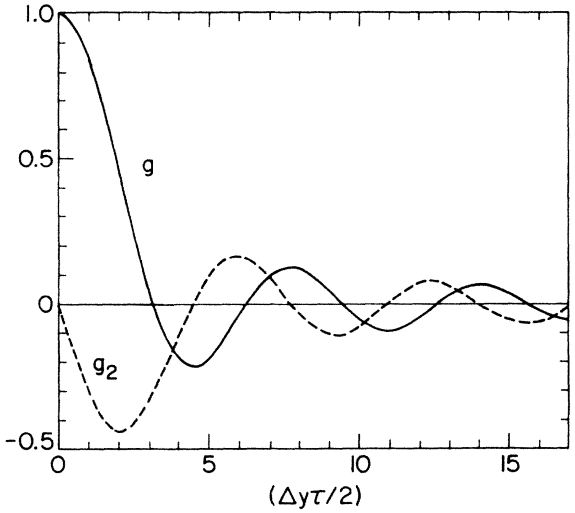

FIG. 2. The functions g and g_2 as a function of their argument $(\Delta y\tau/2)$.

$y\rightarrow 0$. The additional dependence on wavelength through Δy in Eq. (29b) then causes B_2 to approach zero in the limit of long wavelengths. In Fig. 4, the related diffraction pattern for the observed brightness is shown.

Perhaps the most qualitatively significant feature is in Fig. 3 where it can be seen that the amplitude of K has not decreased appreciably at angles t_c that are considerably greater than unity. This leads to an order-of-magnitude or more increase over the usual estimate for the probability for a mass to be close enough to a particular line of sight to have an appreciable effect. With regard to the magnitude of the influence of lensing as measured by $B_2/B_0=(K\Delta y/2)$, bandwidths in the neighborhood of 1% are feasible. Values for K near unity from Fig. 3 would then lead to $B_2/B_0\simeq\frac{1}{100}$. We will return to the issue of the requirement on source size.

III. WKB SOLUTION OF THE WAVE EQUATION

When the parameter $y\gg 1$, evaluation of $\Gamma(\tau)$ based on the full solutions of Sec. II B becomes numerically difficult. Of course, at large y the accuracy of geometrical optics improves and a WKB approximation can be expected to be an adequate treatment for interference phenomena. The basic approximation is in expressing the intensity at location x due to a point source on the axis according to Eq. (32). This form is commonly used in optics when two beams intersect[8] and, except for improvements noted below, is essentially the same as used by Schneider and Schmid-Burk.[3]

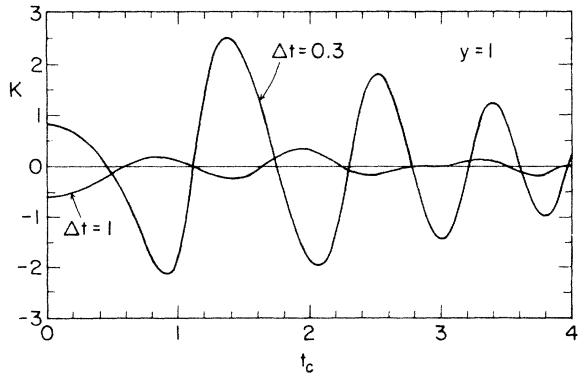

FIG. 3. The quantity K for $y=1$ as a function of the angular location of the source as specified by t_c. The source is treated as a uniform circular disk with an angular diameter $2\Delta t$.

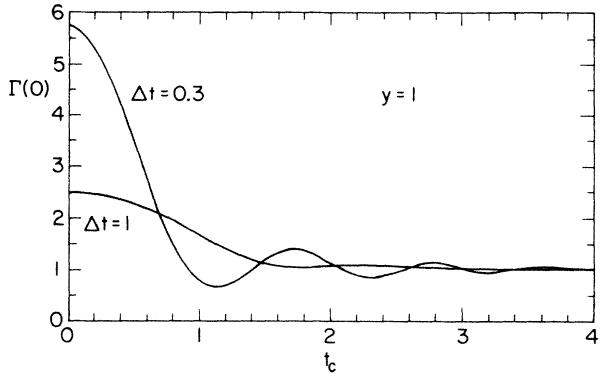

FIG. 4. The brightness of the source divided by the brightness without lensing as a function of the angular location of the center t_c and angular diameter $2\Delta t$ of the source (a uniform circular disk).

A. Formulation

By considering the radiation that passes on opposite sides of the lensing mass as separate rays in geometrical optics, it is natural in the WKB limit to make the approximation in Eq. (24) that

$$R^2\psi^*(x)\psi(x)=I_1(x)+I_2(x)+2[I_1(x)I_2(x)]^{1/2}\cos[P_g(x,y)+\delta]\ . \tag{32}$$

Here, I_1 and I_2 are the amplification factors for the two images, P_g is the phase delay due to the difference in the two paths defined by geometrical optics, and δ is the phase correction. The amplitude factors are the Liebes-Refsdal[9] solutions

$$I_1(x)=\tfrac{1}{4}(2+\xi+\xi^{-1}) \tag{33a}$$

and

$$I_2(x)=\tfrac{1}{4}(-2+\xi+\xi^{-1})\ , \tag{33b}$$

where

$$\xi=(1+4/x)^{1/2}\ . \tag{33c}$$

The phase delay P_g can be calculated from the time delay[10]

$$P_g\equiv\omega T_g$$

$$=k\int_0^{\theta}(\theta_1+\theta_2)\frac{r(r-r_0)}{r_0}d\theta \tag{34a}$$

$$=y\left[(x^2+4x)^{1/2}+2\ln\left[\frac{x+2+(x^2+4x)^{1/2}}{2}\right]\right] \tag{34b}$$

$$\equiv y\tau_x \ , \tag{34c}$$

where the deflection angles θ_1 and θ_2 are by geometrical optics

$$\theta_1=\theta_0[\tfrac{1}{2}x^{1/2}+(1+x/4)^{1/2}] \tag{35a}$$

and

$$\theta_2=\theta_0[-\tfrac{1}{2}x^{1/2}+(1+x/4)^{1/2}] \ . \tag{35b}$$

Let us compare the approximate form in Eq. (32) with the full form given in Eq. (22).

When $x \ll 1$, the confluent hypergeometric function is approximated accurately by the Bessel function:

$$F_c(iy,1,iyx)\simeq J_0(2y\sqrt{x}\,) \ . \tag{36}$$

The asymptotic form of the Bessel function is

$$J_0(2y\sqrt{x}\,)\sim\left[\frac{1}{\pi y}\right]^{1/2}x^{-1/4}\cos\left[2y\sqrt{x}-\frac{\pi}{4}\right] \tag{37}$$

when $2y\sqrt{x} \gg 1$. Hence, for $y \gg 1$,

$$R^2\psi^*\psi=F^*F\simeq x^{-1/2}\left[1+\cos\left[4y\sqrt{x}-\frac{\pi}{2}\right]\right] \ . \tag{38}$$

A comparison of this expression with that in Eq. (32) (using $I_1\sim I_2\sim x^{-1/2}$ and $P_g\sim 4y\sqrt{x}$ which are valid when $x \ll 1$) yields

$$\delta=-\frac{\pi}{2} \ . \tag{39}$$

When $yx \gg 1$, the confluent hypergeometric function can be expressed as the sum of two waves.[5]

$$F_c(iy,1,iyx)\simeq\frac{\exp\left[-iy\ln(yx)-\frac{\pi}{2}y\right]}{\Gamma(1-iy)}+\frac{\exp\left[iy\ln(yx)-\frac{\pi}{2}y+iyx\right]}{\Gamma(1+iy)x} \ . \tag{40}$$

The phase difference between the waves is

$$P_d=yx+2y\ln(yx)+\delta' \ , \tag{41}$$

where

$$e^{+i\delta'}=-\Gamma(-iy)/\Gamma(iy) \ . \tag{42}$$

For large y

$$\delta'\simeq-\frac{\pi}{2}+2y-2y\ln y \tag{43}$$

then

$$P_d\simeq-\frac{\pi}{2}+2y+yx+2y\ln x \ . \tag{44}$$

Comparing this with Eq. (34b) in the limit that $x \gg 1$ also yields

$$\delta=-\frac{\pi}{2} \ . \tag{45}$$

We thus have reason to believe that Eq. (32) with $\delta=-\pi/2$ is quite a good approximation for calculating the intensity distribution in most of the relevant range of x.

However, when x is near zero, the approximation (38) is no longer valid. It is still convenient to separate the intensity into the average (I_1+I_2) and the oscillating term which is proportional to $(I_1I_2)^{1/2}$. The oscillating parts can be written

$$F^*F-(I_1+I_2)\simeq 2\sqrt{I_1I_2}[2\pi y\sqrt{x}\,J_0{}^2(2y\sqrt{x}\,)-1] \ , \tag{46}$$

where we have used $I_1\simeq I_2\simeq x^{-1/2}$. We define

$$f(u)=\pi u J_0{}^2(u)-1 \tag{47}$$

and find that for convenience $f(u)$ can be approximated accurately by

$$f(u)\simeq\begin{cases}\cos\left[2u-\frac{\pi}{2}\right]+\cos\left[\frac{\pi}{2.6}u-\frac{\pi}{2}\right]-1 & \text{for } u\le 1.3 \ , \\ \cos\left[2u-\frac{\pi}{2}\right] & \text{for } u\ge 1.3 \ .\end{cases} \tag{48}$$

This approximation is used instead of Eq. (32) for the relevant regime $(2y\sqrt{x}\le 1.3)$ in the numerical calculations presented in Sec. III B. The function $f(u)$ becomes negative at $u\le 0.35$. This influences the evaluation of the integral around $2y\sqrt{x}\le 0.35$. The need to modify the expression (32) near $x=0$ reflects the general result that the effects of diffraction are severe near a caustic even when more approximate treatments are valid at other locations.

B. Evaluation of the properties of the radiation for objects of finite size

In the WKB limit, it is convenient to express the autocorrelation function obtained from the evaluation of Eq. (3) in the form

$$\Gamma(\tau)=[B_0(\tau)+B_1(\tau)]\cos(y_0\tau)+B_2(\tau)\sin(y_0\tau) \ , \tag{49}$$

which is analogous to that of Eq. (28). For much of the range of x that is of interest, the approximation of Eq. (32) is valid and the explicit expressions for the functions in Eq. (49) in this regime are

$$B_0(\tau)=\tfrac{1}{4}\theta_0^2 g(\tau)\int L(x,\alpha)[I_1(x)+I_2(x)]dx\,d\alpha\ , \tag{50}$$

$$B_1(\tau)=\tfrac{1}{4}\theta_0^2\int [I_1(x)I_2(x)]^{1/2}L(x,\alpha)\cos(y_0\tau_x+\delta)[g(\tau_x-\tau)+g(\tau_x+\tau)]dx\,d\alpha\ , \tag{51}$$

and

$$B_2(\tau)=\tfrac{1}{4}\theta_0^2\int [I_1(x)I_2(x)]^{1/2}L(x,\alpha)\sin(y_0\tau_x+\delta)[g(\tau_x-\tau)-g(\tau_x+\tau)]dx\,d\alpha\ . \tag{52}$$

The functions L and g have the same meaning as in Sec. II, and τ_x is the time delay as specified by Eq. (34c) for a point on the source and the point of observation which are related by the variable x. Thus the effect of bandwidth, which is specified by the dimensionless quantity Δy, is again contained in the function g. In the regime where Eqs. (46) and (48) specify the radiation, $\Gamma(\tau)$ can be expressed in the same form as in Eq. (49). Although B_0, B_1, and B_2 are of slightly different form in this case, they retain essentially the same dependence on $g(\tau)$ and $g(\tau_x\pm\tau)$ as in Eqs. (50)—(52). These expressions for B_0, B_1, and B_2 are given in the Appendix.

Here $B_0(\tau)$ is determined from the integrated amplification factors alone and contains no effects of the coherence caused by gravitational lensing. The observed brightness $\Gamma(0)$ is, from Eq. (49), $[B_0(0)+B_1(0)]$. The intensity resulting in the approximation of geometrical optics is simply $B_0(0)$ whereas the $B_1(0)$ term represents the interference that produces the undulations of the diffraction pattern.

In general, the terms B_1 and B_2 represent the effects of interference. The time delay caused by the lensing can be assessed observationally (at least in principle) by finding the position of the peak of $([B_1(\tau)]^2+[B_2(\tau)]^2)$. For $B_0(\tau)$ the maximum is at $\tau=0$. In contrast, the maximum occurs at $\tau=\tau_x$ for the contribution to $([B_1(\tau)]^2+[B_2(\tau)]^2)$ from the emission in the neighborhood of a point on the source specified by the variable x. This maximum is determined by the function $g(\tau_x-\tau)$ in Eqs. (51) and (52). Although the contributions from a number of points with a range of values for τ_x are summed in the integrals of Eqs. (51) and (52) for a finite source, the largest contribution comes from the part of the source closest to the line between the lens and the observer (that for which x is smallest). Here, $(I_1I_2)^{1/2}$ reaches its peak value rapidly and the contributions from the other regions on the source tend to be less important because of the oscillations in $\cos(y_0\tau_x+\delta)$ and $\sin(y_0\tau_x+\delta)$. When a part of the source is on the lens-observer line (that is, at $x=0$), the maximum in $([B_1(\tau)]^2+[B_2(\tau)]^2)$ is then near $\tau=0$ because $\tau_x=0$ for the dominant contribution. Other considerations aside, a determination of the time delay is facilitated by a maximum in $([B_1(\tau)]^2+[B_2(\tau)]^2)$ that is sharp. This is determined by the bandwidth, which for a sharp maximum must satisfy

$$\Delta\omega T_c=\Delta y\tau_c\gtrsim 1\ , \tag{53}$$

where T_c (or τ_c in our dimensionless units) is the time delay associated with the position on the source closest to the line defined by the lensing mass and the observer.

For the validity of the WKB approximation on which this section is based, it is necessary that $y_0\gg 1$. However, as y_0 increases, the magnitude of B_1 and B_2 is reduced because of the integration involving $\cos(y_0\tau_x+\delta)$ and $\sin(y_0\tau_x+\delta)$. Observational instruments for radio frequencies ordinarily function at bandwidths $\Delta y/y_0\ll 1$. Together with the foregoing consideration that smaller values of y_0 are preferred for the magnitudes of B_1 and B_2, it then follows that $\Delta y\lesssim 1$ is probably of most practical interest. When the bandwidth is small enough—that is, when $\Delta y\ll 1/\tau_x$—Eqs. (50)—(52) indicate that

$$B_0(\tau),B_1(\tau)\gg B_2(\tau) \tag{54}$$

and in the extreme $B_1(\tau)$ is approximately proportional to $g(\tau)$ so that

$$\Gamma(\tau)\simeq\Gamma(0)g(\tau)\cos(y_0\tau)\ . \tag{55}$$

The results of numerical calculations are now presented in several figures to indicate more quantitatively the nature of $\Gamma(\tau)$ and its dependence on the various parameters. In Fig. 5 we illustrate that $B_1(\tau)$ tends to vary in an oscillatory manner with the relative angular location of the source, the lensing mass, and the observer. Note that a particular value for the τ at which to evaluate $B_1(\tau)$ must be chosen for Fig. 5. We have chosen a value at which $B_1(\tau)$ would *a priori* be expected to peak. Examples of the contributions to the autocorrelation function by the terms due to wave effects are presented in Figs. 6(a) and 6(b) for the qualitatively different geometries which are determined by whether or not a part of the source is

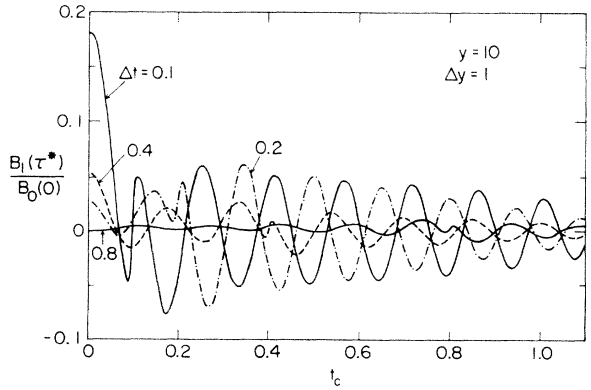

FIG. 5. The ratio $B_1(\tau^*)/B_0(0)$ as a function of the angular location t_c of the center and angular diameter $2\Delta t$ of the source (uniform circular disk) for $y=10$ and $\Delta y=1$. The values chosen for τ^* are $\tau^*=0$ when $\Delta t\geq\tau_c$ and $\tau^*=\tau_x$ for $x=t_c^2$ when $\Delta t<t_c$.

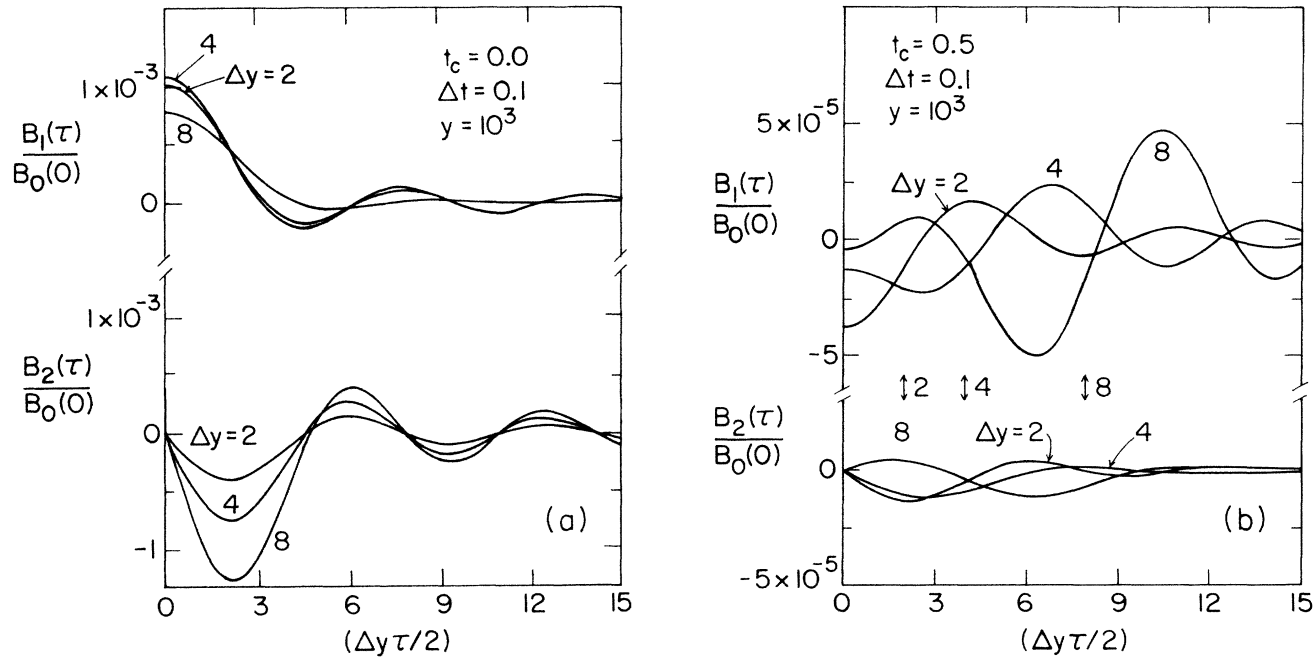

FIG. 6. The ratios $B_1(\tau)/B_0(0)$ and $B_2(\tau)/B_0(0)$ vs $(\Delta y\tau/2)$ for $y=1000$ and $\Delta t=0.1$ for various bandwidths Δy; (a) $t_c=0$, (b) $t_c=0.5$. In (b) the time delays $(\Delta y\tau_x/2)$ for $x=t_c^2$ are indicated by the arrows (source is a uniform circular disk).

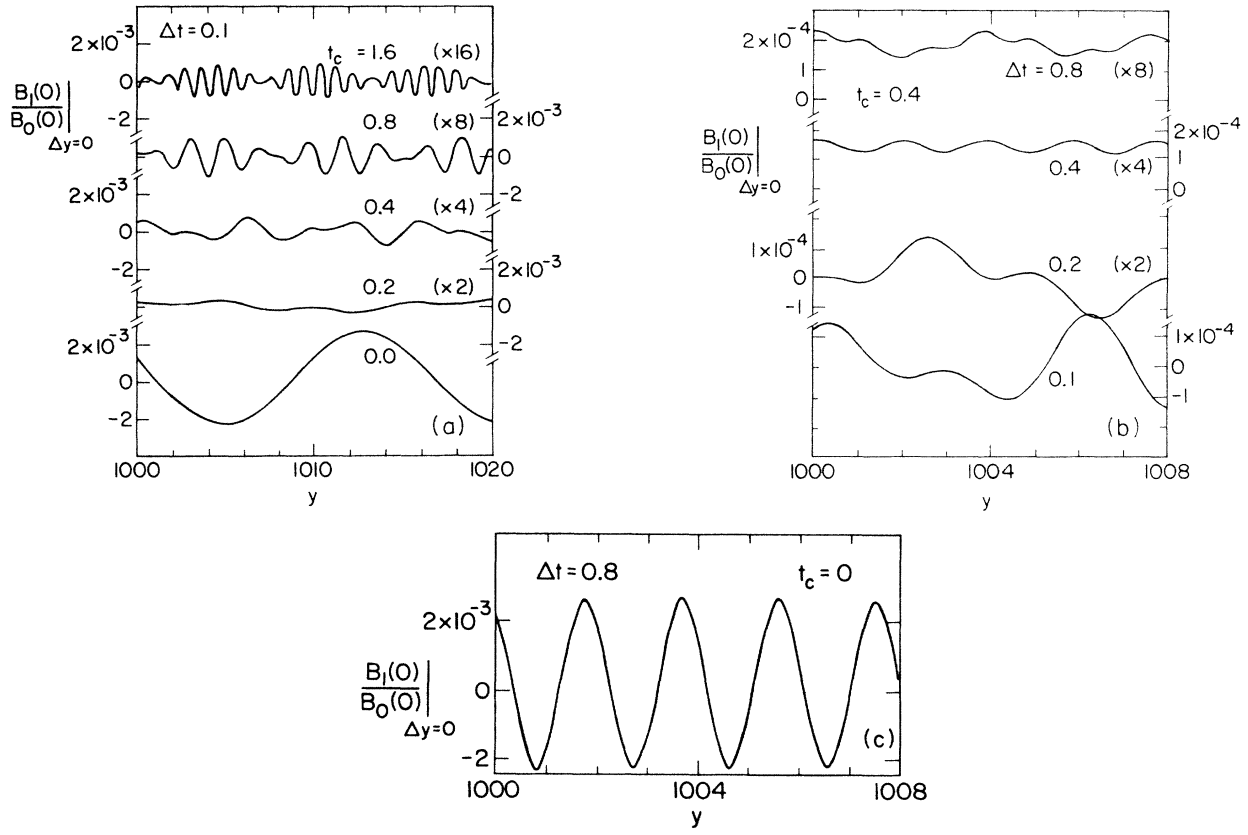

FIG. 7. The ratio $B_1(0)/B_0(0)$ in the monochromatic $(\Delta y=0)$ limit as a function of y near $y=1000$ for a source given by a uniform circular disk; (a) for fixed source size $\Delta t=0.1$ and several locations t_c for the center of the source, (b) for fixed source location $t_c=0.4$ and several sizes Δt for the source (note that all curves except the lowest have been multiplied by various powers of two in order to place the curves in each figure on a common scale), (c) for $t_c=0$ and $\Delta t=0.8$.

directly behind the lensing mass (i.e., at $\theta=0$). For comparison, the variation of $B_0(\tau)$ is shown explicitly by $g(\tau)$ in Fig. 2. In most cases, the peaks of the wave effects in Figs. 6(a) and 6(b) do not occur exactly at the time delays for the point on the source nearest $\theta=0$ or for the central point. Examples to illustrate the variation of the brightness with frequency are obtained for Figs. 7(a) and 7(b) by computing $\Gamma(0)$ in the monochromatic (i.e., $\Delta y \rightarrow 0$) limit. Two characteristic periodicities, evident most clearly in Fig. 7(a), are present in the variations of $\Gamma(0)$ with y. The more rapid variation in this figure is associated with the time difference between the two rays whereas the slower variation is associated with the size of the source.

Finally, Figs. 8 and 9 are presented to indicate the gross variation of the wave effects with the angular location and with the size of the source over a wide range of values for the relevant parameters. Because it is most convenient to calculate B_1 at a particular value of τ, some scatter is introduced into these figures by the tendency for B_1 to oscillate. The general expectation that B_1/B_0 decreases rapidly beyond $\theta \simeq \theta_0$ can, nevertheless, be seen to be supported by Fig. 8. The scatter is less important in Fig. 9 be because the source is centered at $\theta=0$ and $B_1(0)$ is evaluated. In Fig. 9, calculations are also presented for sources represented by circular disks in which the brightness decreases as a Gaussian function of the angle from the center of the disk ($\Delta\theta$ in this case is the half-width at $1/e$ of the peak brightness). When $\Delta t \gtrsim 1$, a variation with approximately $(\Delta t)^{-2}$ is indicated in Fig. 9 for the relative importance of wave effects. This reduction is essentially the dilution due to radiation coming from angles beyond θ_0 and which is largely unaffected by the lensing mass. A variation with $1/y$ is also suggested in Fig. 9 for wave effects—at least for large sources.

IV. DISCUSSION

In considering whether wave effects in gravitational lensing might be detectable or can be utilized to place useful limits on dark matter in the Universe, it is clear that the angular size of the available background sources of sufficient brightness probably is the key issue. Although a detailed discussion of instrumental capabilities and possible configurations or of the astronomical data is well beyond the intent of this study, some orientation may be appropriate. Based on very long base line interferometry (VLBI), studies of interplanetary and interstellar scintillation, and limits for synchrotron-Compton emission,[11] there is no evidence as yet for extragalactic continuum radio sources with angular sizes smaller than about 10^{-4} arcsec. Within our Galaxy, pulsars and radio stars have smaller angular dimensions than do the extragalactic sources. They are, however, weak. In addition to continuum sources, intense spectral line radiation is emitted by astrophysical OH ($\lambda=18$ cm) and H_2O ($\lambda=1.3$ cm) masers associated with molecular clouds in our own Galaxy. These masing regions are composed of a large number of small components. For H_2O masers, hundreds of components having linear dimensions of roughly 10^{13} cm ($\simeq 10^{-4}$ arcsec at 10 kpc) are indicated.[12] Strong OH (Ref. 13) and H_2O (Ref. 14) masers have recently been detected in other galaxies, and also might provide useful background sources in surveys for gravitational lensing if they are composed of similarly small components.

From Eq. (1) and the results of our calculations, the presence of masses down to $M \simeq 10^{-2} M_0$ at representative distances within our own Galaxy can be examined without significant reduction in sensitivity (i.e., in B_1/B_0) due to source size by utilizing the extragalactic, continuum sources with angular sizes of about 10^{-4} arcsec. Because only about 10^{-6} of the randomly chosen directions might be expected to have a lensing mass associated with our Galaxy that is within an angle θ_0 of the line of sight, it would be necessary to study a large number of independent directions. Because of the rotation of the Galaxy and other motions, Earth and a lensing mass of about 10^{-2} M_0 move relative to each other by an angle θ_0 in typically one day. The quantity B_1 then varies on a time scale of roughly $(1/y)$ days, or about 1 min for radiation at wavelengths of 10 cm. Considering lensing masses outside of our Galaxy tends to increase the probability for a lens to be within an angle θ_0 of a source. Unless sources significantly smaller than 10^{-4} arcsec are found, however, the magnitude of the wave effects (as measured by B_1) in extragalactic lensing by a single mass will be reduced because of the size of the source as indicated in Fig. 9. For lensing masses near the plane of our own or other galaxies, the effects of electron scintillation may not be negligible. We will consider electron scintillation in a separate study. When the probability for lensing of a point source is near unity, the effect of multiple lenses must also be considered.

In summary, the methods developed here to extend the WKB treatment to the situation in which a part of the source is on the line between the lens and the observer make it possible to extend considerably the range of relevant situations in which the importance of wave effects can be assessed. In fact, this is the geometry for which the effects tend to be greatest. No strong peak that can be associated with a single time delay is found in the autocorrelation function for any of the parameters considered. When the observer, source, and lens are at least partly aligned, the wave effects in the autocorrelation function are, however, considerably closer to the form of the unaltered function than in the case where there is no alignment. Wave effects are shown to introduce an oscillatory frequency dependence into the amplified brightness of the source whereas the amplification is independent of frequency in the approximation of geometrical optics. For sources larger than θ_0, wave effects can be seen to decrease approximately as (θ_0/angular size of source). When the influence of diffraction is large ($y \lesssim 1$), the influence of the lens on certain properties of the radiation does not decrease appreciably until $\theta \gg \theta_0$ is reached. The probability for lensing effects along a randomly chosen line of sight is then greatly increased. Very small sources are necessary, however, for the effect to be significant.

ACKNOWLEDGMENT

This research has been supported in part by a National Science Foundation Grant No. AST82-16723.

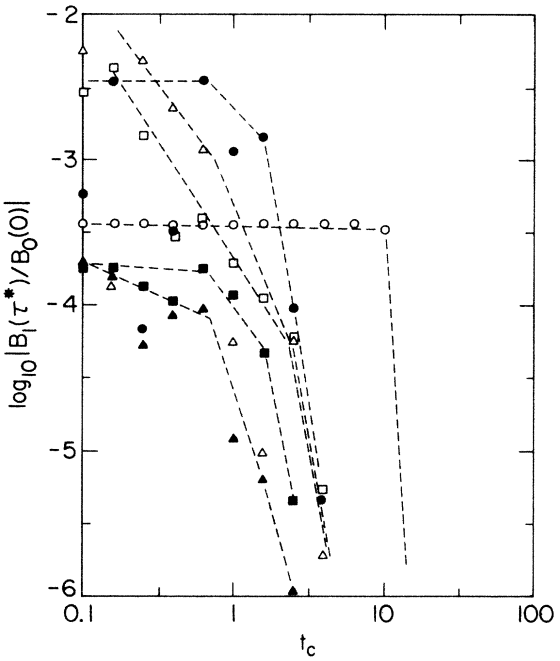

FIG. 8. The ratio $|B_1(\tau^*)/B_0(0)|$ as a function of angular location t_c for the center of the source (uniform circular disk) for bandwidth $\Delta y=1$, and for various values of y and source size Δt (τ^* has the same meaning as in Fig. 5). Symbols: filled triangles, $y=1000$ and $\Delta t=0.1$; open triangles, $y=1000$ and $\Delta t=0.01$; filled squares, $y=100$ and $\Delta t=1$; open squares, $y=100$ and $\Delta t=0.1$; filled circles, $y=10$ and $\Delta t=1$; open circles; $y=10$ and $\Delta t=10$. Dashed lines are only to guide the eye.

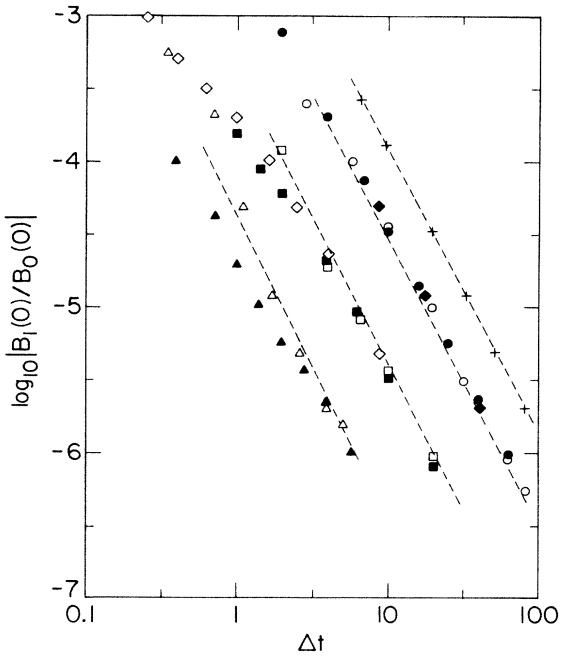

FIG. 9. The ratio $|B_1(0)/B_0(0)|$ as a function of source size Δt when the source is centered directly behind the lensing mass ($t_c=0$). Symbols, for a uniform circular disk source: filled triangles, $y=1000$ and $\Delta y=10$; open triangles, $y=1000$ and $\Delta y=1$; filled squares, $y=100$ and $\Delta y=10$; open squares, $y=100$ and $\Delta y=1$; filled circles, $y=10$ and $\Delta y=2$; open circles, $y=10$ and $\Delta y=1$; crosses, $y=3$ and $\Delta y=0.3$. Additional symbols, for a circular source with a Gaussian decrease in brightness from the center: open diamonds, $y=100$ and $\Delta y=1$; filled diamonds, $y=10$ and $\Delta y=1$. Dashed lines are only to guide the eye.

APPENDIX

When part of the source is at $x=0$ so that it is necessary to use Eq. (48), the following substitutions must be made for B_0, B_1, and B_2 in Eq. (49):

$$B_0(\tau)\rightarrow B_0(\tau)-\tfrac{1}{2}\theta_0^2 g(\tau)\int_0^{x'}[I_1(x)I_2(x)]^{1/2}L(x,\alpha)dx\,d\alpha\ , \tag{A1}$$

$$B_1(\tau)\rightarrow B_1(\tau)+\tfrac{1}{4}\theta_0^2\int_0^{x'}\{[I_1(x)I_2(x)]^{1/2}L(x,\alpha)\cos(y_0\tau'_x+\delta)[g(\tau'_x-\tau)+g(\tau'_x+\tau)]\}dx\,d\alpha\ , \tag{A2}$$

and

$$B_2(\tau)\rightarrow B_2(\tau)+\tfrac{1}{4}\theta_0^2\int_0^{x'}\{[I_1(x)I_2(x)]^{1/2}L(x,\alpha)\sin(y_0\tau'_x+\delta)[g(\tau'_x-\tau)-g(\tau'_x+\tau)]\}dx\,d\alpha\ . \tag{A3}$$

In these substitutions, the $B_0(\tau)$, etc., on the right-hand side of the arrow refer to those given by Eqs. (50)—(52) and, approximately

$$x'=\left[\frac{1.3}{2y_0}\right]^2 \tag{A4}$$

and

$$\tau'_x=\frac{\pi\sqrt{x}}{1.3}\ . \tag{A5}$$

[1]See, for example, K. Chang and S. Refsdal, Nature (London) **282**, 561 (1979); C. R. Canizares, *ibid.* **291**, 620 (1981); J. R. Gott, Astrophys. J. **243**, 140 (1981); P. Young, *ibid.* **244**, 756 (1981); J. P. Ostriker and M. Vietri, Nature (London) **318**, 446 (1985).

[2]A. V. Mandzhos, Pis'ma Astron. Zh. **7**, 387 (1981) [Sov. Astron. Lett. **7**, 213 (1981)].

[3]P. Schneider and J. Schmid-Burk, Astron. Astrophys. **148**, 369 (1985).

[4]S. Deguchi and W. D. Watson, Astrophys. J. (to be published).

[5]See, e.g., L. D. Landau and E. M. Lifshitz, *Quantum Mechanics—Non-Relativistic Theory,* 3rd ed. (Pergamon, Oxford, 1975).

[6]Compare R. A. Matzner, J. Math. Phys. **9**, 163 (1986).

[7]A. Ishimaru, *Wave Propagation and Scattering in Random Media* (Academic, New York, 1978, Vol. 2), p. 440. Note that this application of the transformation is to a slightly different geometry and, hence, has a different appearance.

[8]See, e.g., M. Born and E. Wolfe, *Principles of Optics,* 5th ed. (Pergamon, Oxford, 1975).

[9]S. Liebes, Phys. Rev. B **133**, 835 (1964); S. Refsdal, Mon. Not. R. Astron. Soc. **128**, 295 (1964).

[10]V. Borgeest, Astron. Astrophys. **128**, 162 (1983); R. Kayser and S. Refsdal, *ibid.* **128**, 156 (1983).

[11]See, e.g., K. I. Kellerman, and I. I. K. Pauliny-Toth, Annu. Rev. Astron. Astrophys. **19**, 373 (1981).

[12]R. C. Walker, D. N. Matsakis, and J. A. Garcia-Barreto, Astrophys. J. **255**, 128 (1982).

[13]See, e.g., W. A. Baan, P. A. D. Wood, and A. D. Haschick, Astrophys. J. **260**, L49 (1982).

[14]See, e.g., F. F. Gardner and J. B. Whiteoak, Mon. Not. R. Astron. Soc. **201**, 12P (1984); M. J. Claussen, G. M. Heligman, and K. Y. Lo, Nature (London) **310**, 298 (1984); C. Henkel, R. Gusten, D. Downes, C. Thum, T. L. Wilson, and P. Bierman, Astron. Astrophys. **141**, L1 (1984).